

Appendix 2

PREPARATION AND IMAGING OF SIMS MOUNTS

All experimental charges were mounted, together with the corresponding garnet reference material, in the central part of 25.4 mm epoxy discs. The integrity of the diffusion interface was checked either by a Leica DM6000_M automated microscope in reflected light mode or by SEM imaging in Backscattered Electron (BSE) and CL modes (Figs. 1, 2, 3). Prior to analysis by SHRIMP, mounts were coated with 15 nm of aluminum or gold after chemical cleaning. Prior to analysis with a CAMECA IMS-1280, mounts were coated with ~60 nm thick gold. Samples were kept in a vacuum oven at 60 °C for at least 48 h before being introduced into the instruments.

For NanoSIMS analyses, crystals were removed from their epoxy mounts and pressed into indium (preferable to epoxy for maintaining ultra-high vacuum $\sim 10^{-8}$ Pa) in 25 mm aluminum holders, which were then gold-coated (15 nm).

SHRIMP traverses were imaged with a LEICA DM6000_M automated microscope (Research School of Earth Sciences, ANU) that allowed the average distance of each spot perpendicular from the diffusion interface to be measured. Traverses measured by NanoSIMS were imaged with a JSM-6610A SEM at the Research School of Earth Sciences (ANU) in BSE and Secondary Electron (SE) mode. Traverses measured with a CAMECA IMS-1280 were imaged using a Hitachi S3400 SEM at the Department of Geoscience (UW-Madison) using BSE and SE imaging modes. In addition, traverses in three experimental charges were also imaged in CL mode using a Gatan Pana/CL/F system. Finally, SHRIMP and CAMECA IMS-1280 pits from depth profiling analyses were imaged with a Leica DCM8 confocal microscope (Research School of Earth Sciences, ANU) and a ZYGO white-light

interferometer (Department of Materials Science and Engineering, UW-Madison), respectively, to check their geometry and to measure their depth.

ANALYTICAL METHODS FOR OXYGEN ISOTOPE ANALYSIS

Sensitive High Resolution Ion Microprobe (SHRIMP)

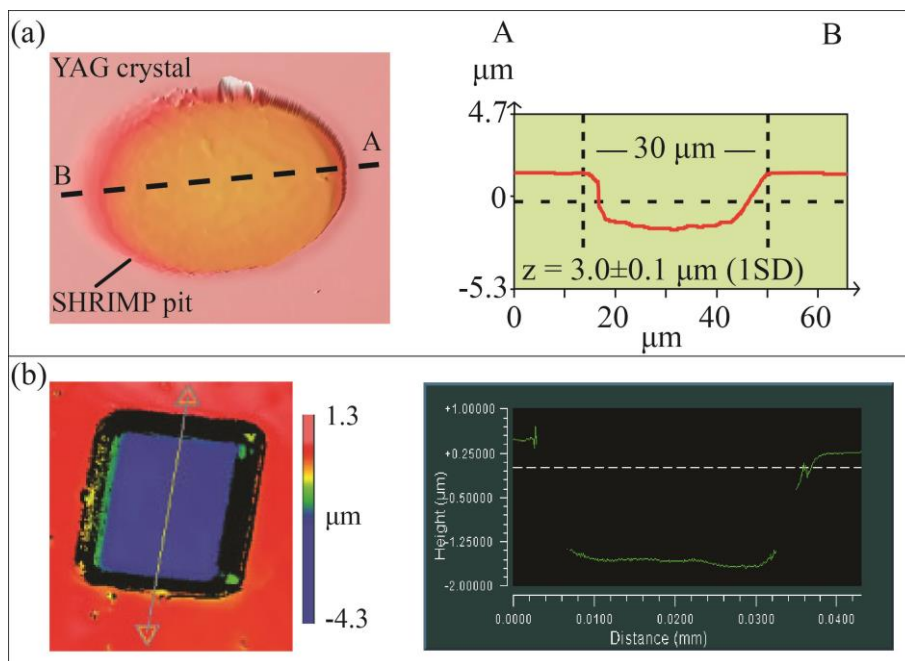
SHRIMP II and SHRIMP SI instruments at the Research School of Earth Sciences, ANU (Ireland et al. 2008) were used both in line-scan and static depth profiling modes to measure $^{18}\text{O}/(^{18}\text{O}+^{16}\text{O})$.

Line-scan analyses were performed with a ~ 2 nA Cs^+ primary ion beam focused to $\sim 10 \times 15$ μm beam footprint on the sample surface, which was pre-sputtered for 60 s before data collection. Background was measured with an integration time of 10 s. Typical count rates were $7.3\text{-}9.3 \times 10^8$ cps for $^{16}\text{O}^-$, whereas for $^{18}\text{O}^-$ they were $1.5\text{-}1.9 \times 10^6$ cps for YAG reference material and $1.4 \times 10^6\text{-}2.1 \times 10^7$ cps for YAG annealed under experimental conditions. The range in $^{18}\text{O}^-$ counts represents the variation from the background to the interface with the ^{18}O -doped matrix. Each analysis consisted of a total counting time of 120 to 240 s resulting from 6 to 12 sub measurements of 10 or 20 s each. The total acquisition time for an $^{18}\text{O}/(^{18}\text{O}+^{16}\text{O})$ profile in line-scan mode varied between 1.5-3.0 h (i.e., 13-28 analytical spots, respectively). The spatial resolution of this analytical setup is limited by the size of the analytical spot (~ 10 μm); hence traverses were performed diagonally to the diffusion interface to increase the number of analytical spots within the diffusion profiles (Fig. 1c, 3d). More than one profile per sample was usually measured to ensure reproducibility of the results.

Depth profiling analysis has the advantage of allowing continuous measurements with depth and analysis of short diffusion profiles (e.g., Hofmann 2014). However, several instrumental effects can distort the shape of diffusion profiles measured in static depth

profiling mode (see Zinner 1980 and Cherniak et al. 2010 for a review). The sputtering rate in the different garnet reference materials was constant (see below). In order to obtain flat-bottomed pits to minimize edge effects, a $\sim 1.5\text{--}2.0$ nA primary beam was enlarged to a spot size of 25×30 μm by focusing on a 200 μm Kohler aperture. The analytical site was sputtered for 30 s before data collection in order to remove the Au or Al coating. Background was measured with an integration time of 20 s. Typical count rates on $^{16}\text{O}^-$ and $^{18}\text{O}^-$ for garnet reference materials were $9.4\text{--}9.9 \times 10^8$ cps and $1.9\text{--}2.0 \times 10^6$ cps, respectively, for all garnet compositions. Each analysis had a total counting time of 30 to 50 min, and consisted of 100 to 150 sub measurements of 20 s each. Depth resolution during depth profiling by SIMS is conventionally described as the distance (Δz) over which a 16% to 84% change in signal is measured when profiling through an ideally sharp interface between two media; if the resulting shape of such an interface profile is approximated by an error function, then $\Delta z = 2\sigma$, where σ is the standard deviation of the corresponding Gaussian resolution function (Hofmann 2000). Depth resolution during depth profiling analysis by SHRIMP was estimated by profiling garnet reference materials coated with an ^{18}O -enriched olivine thin film following the Pulsed Laser Deposition technique described in Dohmen et al. (2002). Depth resolution during depth profiling was on the order of ~ 160 nm (1σ ; Table S4, electronic supplement). More than one profile per sample was usually measured to ensure consistency of the results. Only data obtained from flat-bottomed pits were considered reliable (Fig. A2-1).

Figure A2-1. (a) 3D confocal microscope image of a flat-bottomed SHRIMP pit with corresponding cross-section. The asymmetry of the pit is due to the 45° incident angle of the primary ion beam. (b) 3D image and corresponding cross section, acquired with a white-light interferometer, of a 30 μm square raster area formed by depth profiling with a CAMECA IMS-1280.



Nanoscale Secondary Ion Mass Spectrometry (NanoSIMS)

A CAMECA NanoSIMS N50L secondary ion mass spectrometer (Hoppe et al. 2013) within the Center for Advanced Surface Analysis at the University of Lausanne, was used in line-scan mode to measure $^{18}\text{O}/(^{18}\text{O}+^{16}\text{O})$ profiles that were in the 5-30 μm length range, hence too short for line-scan or too long for depth profiling by SHRIMP. Some experimental charges previously analyzed by SHRIMP were reanalyzed with the NanoSIMS to crosscheck the results. Oxygen isotopes were measured as negative secondary ions by using a Cs^+ primary ion beam focused to ~ 100 nm with impact energy of 16 keV. Primary beam currents in the range 1.2-4.7 pA yielded analytical precisions of ~ 1 -2% (1RSD, relative standard deviation) for counting rates of 10^5 cps for $^{16}\text{O}^-$ and 10^2 cps for $^{18}\text{O}^-$ in the garnet reference material. Line scans were performed in beam-controlled mode (Kilburn and Wacey 2014). Presputtering along the selected line-scan (Fig. 3a) was done for 3 cycles with dwell times of 2 s per pixel using the D1-2 aperture, i.e., with a beam intensity of 4.7 pA and a spot-size of roughly 350 nm. Data were collected along the same line scan over 10 cycles with dwell times of 2 s per pixel and the beam focused to ~ 100 nm. Each analysis lasted for ~ 3 h. $^{27}\text{Al}^-$,

$^{89}\text{Y}^-$, $^{89}\text{Y}^{16}\text{O}^-$ were analyzed simultaneously to $^{16}\text{O}^-$ and $^{18}\text{O}^-$ to monitor transient effects across the interface.

CAMECA IMS-1280

A CAMECA IMS-1280 large radius multicollector secondary ion mass spectrometer at the WiscSIMS laboratory (UW-Madison) was used to measure additional $^{18}\text{O}/(^{18}\text{O}+^{16}\text{O})$ profiles in both line-scan and depth profiling mode. Analytical settings for line-scan analysis were similar to routine oxygen isotope analyses using multi-collection Faraday cup detectors (Kita et al. 2009), except a Cs^+ primary ion beam was focused to $\sim 2 \times 3 \mu\text{m}$ spots with an intensity of $\sim 30 \text{ pA}$. Impact energy of primary ions was 20 keV (+10 kV for primary ions and -10 kV for secondary ions). Secondary ions of $^{16}\text{O}^-$, $^{18}\text{O}^-$ and $^{16}\text{O}^1\text{H}^-$ were collected simultaneously using three Faraday cup detectors. Typical count rates for $^{16}\text{O}^-$, $^{18}\text{O}^-$ and $^{16}\text{O}^1\text{H}^-$ were in the order of $2.0\text{-}4.1 \times 10^7 \text{ cps}$, 4.6×10^4 to $8.5 \times 10^5 \text{ cps}$ and $1.1\text{-}7.8 \times 10^4 \text{ cps}$, respectively. The $^{16}\text{O}^1\text{H}^-/^{16}\text{O}^-$ ratio (hereafter OH/O) measured in experimental charges was corrected for background by subtracting the OH/O value of bracketing YAG reference material. Each analysis lasted $\sim 4 \text{ min}$ including 60 s of pre-sputtering, 120 s of automated centering of the secondary ions and 80 s of data acquisition (20 cycles of 4 s each). Bias, drift and spot-to-spot precision were monitored by bracketing 25-30 analyses in the experimental charges with eight analyses in the YAG reference material ($\delta^{18}\text{O}_{\text{V-SMOW}} = 14.92 \pm 0.25\%$, 2SD, see below) located in the same mount.

Unlike SHRIMP instruments, depth profiling analysis using IMS-1280 SIMS minimizes the edge effects by filtering the secondary ions from the center of rastered areas using physical and electronic gates (Zinner 1980; Van Orman et al. 2014). $^{18}\text{O}/(^{18}\text{O}+^{16}\text{O})$ depth profiling was performed using a +10 kV Cs^+ primary ion beam focused to $\sim 10 \mu\text{m}$ diameter with an intensity of $\sim 2 \text{ nA}$ and raster sizes of 30 and 50 μm square area. An electronic gate of

30% was used, restricting sampling of secondary ions to a central 10 or 15 μm square area on the sample surface for 30 and 50 μm raster, respectively. In addition, the field aperture was set to 2000 or 3000 μm square for 30 and 50 μm raster, respectively, which corresponds to a physical gate of 10 or 15 μm on the sample surface by using transfer optics with $\times 200$ magnifications. Secondary ions of $^{16}\text{O}^-$, $^{18}\text{O}^-$ and $^{16}\text{O}^1\text{H}^-$ were collected simultaneously using three Faraday cup detectors and typical count rates for $^{16}\text{O}^-$ and $^{18}\text{O}^-$ were on the order of 9.0×10^7 to 1.6×10^8 cps and 2.0×10^5 to 1.7×10^7 cps, respectively. Measured OH/O ratios in experimental charges were background corrected by subtracting the average OH/O values measured in YAG and pyrope reference materials during the same session. Counting time per each cycle was 10 s and pre-sputtering time was 30 s or 80 s (for 30 and 50 μm raster, respectively). Depth resolution estimated on the YAG reference material coated with an ^{18}O -enriched olivine thin film was on the order of ~ 20 nm (1σ ; Table S4, electronic supplement).

SPUTTERING RATE

In order to convert sputtering time into depth, the sputtering rate has to be constant (Zinner 1980). This can be investigated by measuring depth profiles of different durations and by plotting the sputtering times against the depth of the pits: if the sputtering time is constant, a linear correlation will be observed (e.g., Giletti et al. 1978).

Sputtering rates in the different garnet reference materials (i.e., YAG, Prp-1, and Grs-2) were investigated by performing depth profiles of different durations (i.e., total sputtering time between 716-2937 seconds). The depth of the SHRIMP pits was measured with a Leica DCM8 confocal microscope at the Research School of Earth Sciences (ANU). The linear relationship between sputtering time and depth of the SHRIMP pits (Fig. A2-2) suggests that sputtering rates are constant under the analytical conditions used in this study. Despite the primary ion flux varying between 1.5 and 1.8 nA during two different analytical sessions on

YAG, calculated sputtering rates were comparable within error (1.8 ± 0.2 nm/s and 2.0 ± 0.1 nm/s, respectively). A comparable sputtering rate of 1.5 ± 0.2 nm/s was calculated for Prp-1 and Grs-2 under similar analytical conditions.

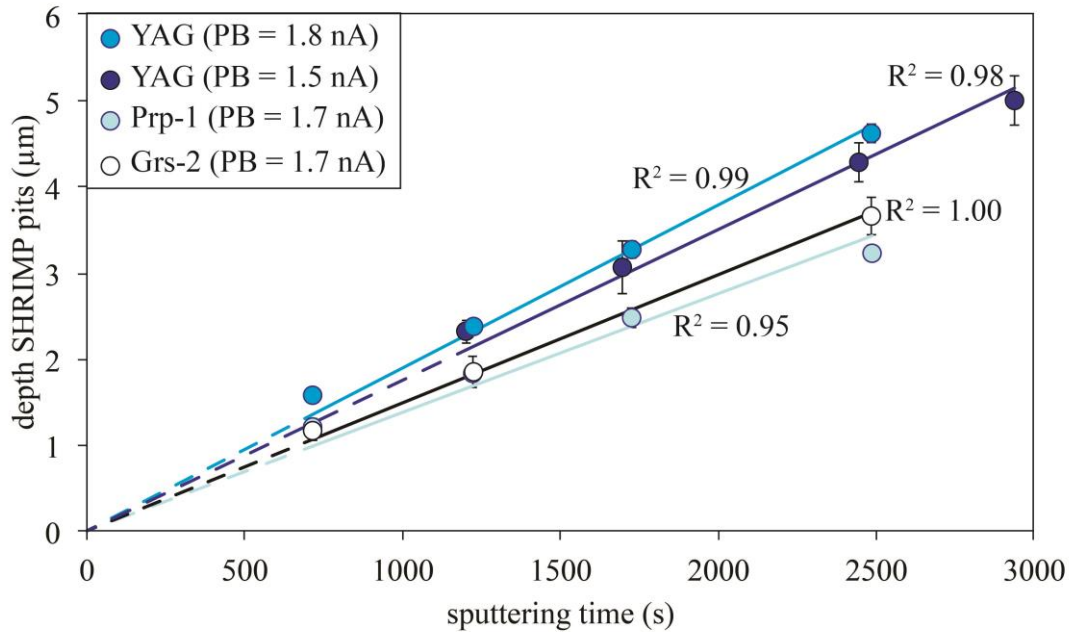


Figure A2-2. Diagram showing the linear correlation between sputtering time and depth of the SHRIMP pits, suggesting constant sputtering rates for YAG, Prp-1, and Grs-2. The intensity of the primary ion beam (PB) is also indicated. A comparable sputtering rate was calculated for YAG under different primary ion beam intensities.

YAG REFERENCE MATERIAL FOR SIMS OXYGEN ISOTOPE ANALYSIS

Bulk oxygen isotope measurements of the YAG starting material used for experiments were performed with a 32 W CO₂ laser fluorination system coupled with a triple-collecting Finnigan/MAT 251 mass spectrometer at the Stable Isotope Laboratory, UW-Madison (Valley et al. 1995). The UWG-2 garnet reference material (Valley et al. 1995) was analyzed 5 times at the start of, and 2-3 times during, the analytical session. Raw values were corrected using the mean measured value for UWG-2 compared with the recommended value of 5.80‰

V-SMOW for UWG-2 (Valley et al. 1995). The mean correction was +0.1‰, and daily precision averaged $\pm 0.22\%$ (2SD). Bulk oxygen isotope analyses of YAG are shown in Table A2-1.

TABLE A2-1

Sample ID	$\delta^{18}\text{O}_{\text{V-SMOW}}$ (‰)	average $\delta^{18}\text{O}_{\text{V-SMOW}}$ (‰)	2SD (‰)	2SE (‰)
YAG	15.01	14.92	0.25	0.18
YAG	14.83			

Oxygen isotope homogeneity of YAG at the microscale was tested with a CAMECA IMS-1280 at the WiscSIMS lab (UW-Madison). Analytical settings were similar to those reported in Kita et al. (2009) for a Cs^+ primary ion beam with an intensity of ~ 2 nA focused to ~ 10 μm spots. UWG-2 garnet located on a different grain mount was used as bracketing reference material to monitor instrumental bias, spot-to-spot reproducibility and drift. SIMS analyses in a ~ 1 mm^3 YAG crystal relative to UWG-2 are shown in Table A2-2. Spot-to-spot reproducibilities were $\pm 0.8\%$ and $\pm 0.4\%$ (2SD) in YAG and UWG-2 garnet, respectively. The instrumental bias in YAG is significantly larger than that in UWG-2 (i.e., 17.8‰ vs. 1.2‰, respectively).

TABLE A2-2

Analysis ID	$\delta^{18}\text{O}$ ‰ measured	2SE (int.)	$\delta^{18}\text{O}$ ‰ V-SMOW	Bias ‰	^{16}O (Gcps)	IP (nA)	Yield (Gcps/nA)
UWG-2	6.90	0.20			2.64	2.05	1.28
UWG-2	6.92	0.09			2.64	2.05	1.28
UWG-2	7.15	0.13			2.63	2.05	1.28
UWG-2	6.95	0.13			2.62	2.05	1.28
YAG-1	33.36	0.80			0.53	2.08	0.25
YAG-1	33.33	1.03			0.53	2.08	0.25
YAG-1	32.45	1.02			0.51	2.08	0.24
YAG-1	33.20	1.03			0.53	2.07	0.26
YAG-1	33.48	0.90			0.53	2.07	0.26
YAG-1	32.99	0.96			0.52	2.07	0.25
YAG-1	32.59	0.89			0.52	2.07	0.25
YAG-1	32.78	0.92			0.50	2.07	0.24
YAG-1	33.22	1.18			0.50	2.06	0.24
YAG-1	32.37	0.90			0.51	2.06	0.25
<i>average and 2SD</i>	32.98	0.81	14.92	17.79			
UWG-2	6.83	0.20			2.60	2.01	1.29
UWG-2	6.98	0.14			2.60	2.01	1.29
UWG-2	7.17	0.16			2.60	2.02	1.29
UWG-2	7.34	0.11			2.59	2.02	1.28
<i>bracket average and 2SD</i>	7.03	0.35	5.80	1.22			